Nano Research

ISSN 1998-0124 CN 11-5974/O4
https://doi.org/10.1007/s12274-021-3285-3

Research Article

# Monolithic superaligned carbon nanotube composite with integrated rewriting, actuating and sensing multifunctions

Peidi Zhou[1,2,§], Wei Zhang[1,2,§], Luzhuo Chen[1,2] (✉), Jian Lin[1,2], Zhiling Luo[1,2], Changhong Liu[3], and Kaili Jiang[3,4]

[1] *Fujian Provincial Key Laboratory of Quantum Manipulation and New Energy Materials, College of Physics and Energy, Fujian Normal University, Fuzhou 350117, China*
[2] *Fujian Provincial Collaborative Innovation Center for Advanced High-Field Superconducting Materials and Engineering, Fuzhou 350117, China*
[3] *Tsinghua-Foxconn Nanotechnology Research Center, Department of Physics, Tsinghua University, Beijing 100084, China*
[4] *State Key Laboratory of Low-Dimensional Quantum Physics, Department of Physics, Tsinghua University, Beijing 100084, China*
[§] *Peidi Zhou and Wei Zhang contributed equally to this work.*


**Received:** 3 September 2020 / **Revised:** 14 November 2020 / **Accepted:** 7 December 2020

## ABSTRACT

Multifunctionality has become a mainstream trend in the development of smart clothing and flexible wearable devices. Nevertheless, it remains a grand challenge to realize multiple functions, such as sensing, actuating and information displaying, in one single multifunctional material. Here, we present one multifunctional integration strategy by employing monolithic superaligned carbon nanotube (SACNT) composite, which can leverage three different functions through fascinating features of SACNT. Firstly, by using thermochromic dye as a color-memorizing component and SACNT as a photothermal converter, the composite film can be utilized as a flexible rewritable medium. It demonstrates excellent rewriting performances (reversibility > 500 times). Secondly, the composite can be tailored to fabricate an actuator, when its length direction is along the SACNT alignment. The actuator shows a bending-morphing when illuminated by near-infrared light. The morphing is attributed to a large difference in volume change between the SACNT and polymer when the SACNT absorbs the optical energy and heats the composite. Thirdly, owing to the unique anisotropy of SACNT, the composite is easily to be stretched in the direction perpendicular to the SACNT alignment, accompanied by a change in electrical resistance. Therefore, the composite is able to be used as a strain sensor. Finally, we fabricate two smart wearable devices to demonstrate the applications, which realize the functions of human-motion detection (sensing) and rewritable information display (rewriting) simultaneously. This multifunctional SACNT composite is expected to have potential applications in the next-generation wearable devices, smart clothing and so on.

## KEYWORDS

carbon nanotube, actuator, sensor, rewritable media, multifunctional

## 1 Introduction

For the past few years, flexible electronic devices have developed rapidly [1, 2]. Compared with traditional non-stretchable rigid electronics, the properties of flexible electronic devices won't be significantly degraded under tensile and twisting deformation, playing an important role in the field of smart clothing and flexible wearable devices [3, 4]. Among them, actuators [5–7], sensors [8, 9], and color-switching devices have attracted particular attentions [10, 11]. However, many flexible wearable devices currently only have one single function. With the increasing demand on the various functions and lightweight, the functions and volumes of single-functional devices are approaching their limits. Multifunctional materials and devices, which can reduce costs and improve space utilization, are becoming an important direction for future research of flexible wearable devices. Recently, researchers have begun to make progress in this aspect. However, some multifunctional devices are only prepared by combining materials with different functions. For example, a multifunctional sensor that converts pressure and temperature stimuli into two independent electrical signals was proposed [12]. The multifunctional sensor was integrated from piezoelectric and thermoelectric materials. These two signals were generated from two different materials. Meanwhile, most of the multifunctional devices can only achieve two functions. For example, flexible devices with both sensing and actuating functions [13–16], and actuating materials with color-switching functions have been reported [17–19], which extend the functions of actuating materials and are useful in soft robotics. Energy storage devices with color-switching functions have also been developed, in which the color can reflect the state of supercapacitors [20–22]. Material selection and functional design are the difficulties and challenges in realizing multifunctional devices. In terms of material selection, simply stacking multiple materials with different functions will complicate the device system and make it more difficult to manufacture multifunctional devices. It is preferred to make use of different properties of the same material to achieve multiple functions. In terms of functional design, it is difficult to realize a multifunctional material with more than three

Address correspondence to ChenLZ@fjnu.edu.cn

functions, which places great demands on the choice of function and the structure design. What's more, the synergy between the different functions of multifunctional devices is also necessary. Consequently, it remains a grand challenge to realize multiple (> 2) functions, such as sensing, actuating and information displaying, in one single multifunctional material.

Here, we propose one multifunctional integration strategy by employing monolithic superaligned carbon nanotube (SACNT) composite, which can deliver multiple functions through unique features of SACNT. The composite film has a bilayer structure: one layer is mainly composed of SACNT, and the other layer consists of thermochromic dye (TD) and polydimethylsiloxane (PDMS). The SACNT/TD-PDMS composite is capable of realizing three functions respectively. Firstly, it can be used as a rewritable medium. Information or patterns are photoprinted and displayed on the composite film, which demonstrates excellent rewriting performances (reversibility > 500 times and legible time > 6 months). Secondly, the SACNT/TD-PDMS composite can be tailored to fabricate an actuator, when its length direction is along the SACNT alignment. The actuator shows a bending-morphing under near-infrared (NIR) light illumination. Thirdly, the SACNT/TD-PDMS composite is able to be used as a strain sensor, which sustains stretching in the direction perpendicular to the SACNT alignment, accompanied by a change in resistance. Finally, we fabricate a smart glove and a smart armband to demonstrate the applications, which exhibit the functions of human-motion detection and rewritable information display simultaneously. These results prove that multifunctional wearable devices can be achieved by using monolithic SACNT/TD-PDMS composite, which is expected to have potential applications in the fields of rewritable media, artificial muscles, soft robotics and smart clothing.

## 2 Experimental

The highly anisotropic SACNT film was manufactured by a solution-free approach, which has been developed since 2002 [23–26]. Figure 1(a) displays the fabrication process of SACNT/TD-PDMS composite. Firstly, 50 layers of SACNT sheets were pulled out from a SACNT array and coated on a PET substrate. Secondly, the TD and uncured PDMS mixture were uniformly mixed in a mass ratio of 2:8 and coated on the SACNT. The color of the TD will change according to the temperature variation. Finally, the solid-state SACNT/TD-PDMS composite was obtained after curing. The thickness of composite film was 279 μm. More details of experiment are in Note S1 in the Electronic Supplementary Material (ESM).

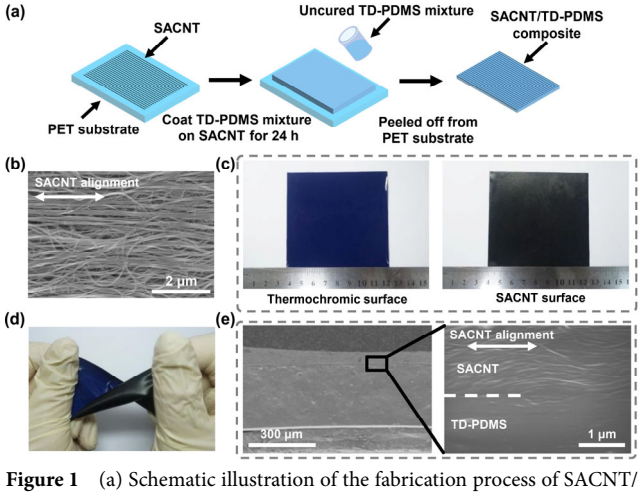


**Figure 1** (a) Schematic illustration of the fabrication process of SACNT/TD-PDMS composite. (b) SEM image showing the surface morphology of SACNT film. (c) Optical photographs of the prepared SACNT/TD-PDMS film: thermochromic surface (left panel), SACNT surface (right panel). (d) Optical photograph showing the flexibility of SACNT/TD-PDMS film. (e) Cross-sectional SEM images of the SACNT/TD-PDMS film.

## 3 Results and discussion

### 3.1 Characterization of SACNT/TD-PDMS composite

SACNT is one of the important components in the SACNT/TD-PDMS composite. The SACNT is flexible, conductive and highly anisotropic, making it ideal for a wide range of flexible electronic devices [25, 27–29]. The scanning electron microscope (SEM) image (Fig. 1(b)) demonstrates the microscopic morphology of SACNTs. It can be seen that the nanotubes were highly anisotropic and well-aligned in the same direction. The appearances of two sides of the SACNT/TD-PDMS composite are shown in Fig. 1(c). The thermochromic layer (TD-PDMS layer) was blue and the SACNT layer was black. Figure 1(d) shows that the SACNT/TD-PDMS composite film was highly flexible, making it applicable for wearable devices. The SEM image of the SACNT surface of the composite is shown in Fig. S1 in the ESM, indicating that the SACNTs are still well-aligned in the same direction after fabrication. Figure 1(e) displays the cross-sectional SEM images of the composite film. The whole thickness of the SACNT/TD-PDMS composite is about 279 μm. The enlarged SEM image shows that the composite has a bilayer structure. One layer is TD-PDMS composite. The other layer is mainly composed of SACNT, while the gaps between the SACNTs are filled by TD-PDMS composite. As the main component of this layer is SACNT, it is still named as "SACNT layer". There is no delamination between the SACNT layer and the TD-PDMS layer, indicating that the two layers are well combined.

The prepared SACNT/TD-PDMS composite is a multifunctional material that can deliver three different functions according to requirements, as shown in Fig. 2. Firstly, by means of light irradiation and low temperature condition, we can easily photoprint and erase patterns on the composite film. Therefore, it demonstrates the function of a rewritable medium and can be used for information display. Secondly, as the SACNT is highly anisotropic, the angle between the length direction of the composite and the SACNT alignment is defined as $\alpha$. When the SACNT/TD-PDMS film is tailored into strips ($\alpha = 0°$), it is an actuator and shows obvious bending-morphing under NIR light irradiation. Finally, the SACNT/TD-PDMS composite is stretchable along the direction perpendicular to SACNT alignment ($\alpha = 90°$), and can be used as a strain sensor. More details will be explained in the following sections.

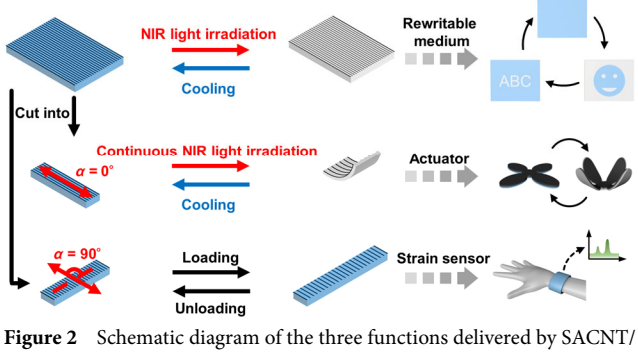


**Figure 2** Schematic diagram of the three functions delivered by SACNT/TD-PDMS composite.

### 3.2 Rewritable performance of the SACNT/TD-PDMS composite

Despite the continuous development of digital technology, we still need a lot of traditional printing materials in our lives. However, most printing materials are used only for one-time reading, and the printing materials after use will cause enormous environmental problems. The rewritable medium is one of the alternative solutions to this problem. The SACNT/TD-PDMS composite can be utilized as a rewritable medium, which is attributed to the thermochromic effect induced by color-memorizing TD. The TD is usually composed of an electron donor, an electron acceptor, and a solvent. Here, crystal violet lactone (CVL) works as the electron donor. Phenolic compound (e.g., bisphenol A) works as the electron acceptor, and aliphatic carboxylic acids (or aliphatic esters) are used as the solvent. The TD is blue under normal conditions. When the temperature of TD is higher than the fusing point of the solvent (> 60 °C), the solvent molecules block the interaction between the electron donor (CVL) and the electron acceptor (developer). Therefore, the color of TD shifts from blue to colorless. Afterwards, the low temperature will make the CVL and the developer recrystallize to a solid-state and restore their interaction, so the color of TD returns to blue. In a word, the thermal-driven phase change mechanism results in the thermochromic effect [30]. The color-memorizing of the SACNT/TD-PDMS composite is owing to the thermochromic layer, while the SACNT provides fast energy conversion from optical energy to heat energy. As shown in Fig. 3(a), customized patterns can be photoprinted on or erased from the SACNT/TD-PDMS film in a facile way. A photomask is placed on the SACNT layer side of the composite. When exposed to NIR light, the exposed positions of the SACNT/TD-PDMS film are heated and the color will be changed. When the light is turned off, the patterns can be remained on the SACNT/TD-PDMS film, so the information can be kept and displayed clearly. Two ways are offered to "erase" the patterns on the rewritable medium. The first way is called "resetting". By placing the SACNT/TD-PDMS film at low temperature (−20 °C) for 10 min, the thermochromic layer can restore the original blue color. Accordingly, operators are able to continue photoprinting patterns on the SACNT/TD-PDMS film by using NIR light again. However, such an erasing method may cause inconvenience, because it needs some patience to wait for the erasing (10 min), and it is discommodious to achieve a low temperature environment (−20 °C) without refrigeration equipment. Therefore, we provide the other fast erasing way—the "deleting" method. By placing the SACNT layer under NIR light, the entire SACNT/TD-PDMS composite will be heated up promptly due to photothermal effect. The remaining portion with blue color on the thermochromic layer will also shift to a colorless state, so the previous printed patterns are deleted instantaneously. If the operators intend to photoprint other patterns on the SACNT/TD-PDMS film, the low-temperature resetting process should be conducted again.

For the purpose of more intuitively investigating the thermochromic properties, a TD-PDMS composite film was prepared and tested. The thickness of TD-PDMS film was 270 μm. As shown in Fig. 3(b), the TD-PDMS film had an obvious absorption peak at wavelength of 610 nm, accompanied by blue color of the film appearance. Once its temperature exceeded 60 °C, the color of the TD-PDMS film turned from blue to colorless and the absorption peak vanished. When the TD-PDMS film was cooled to −20 °C, the absorption peak showed up again, and the TD-PDMS film emerged blue color once more. For comparison, the absorption spectrum of the pure PDMS film which had no absorption peak is also demonstrated in Fig. 3(b).

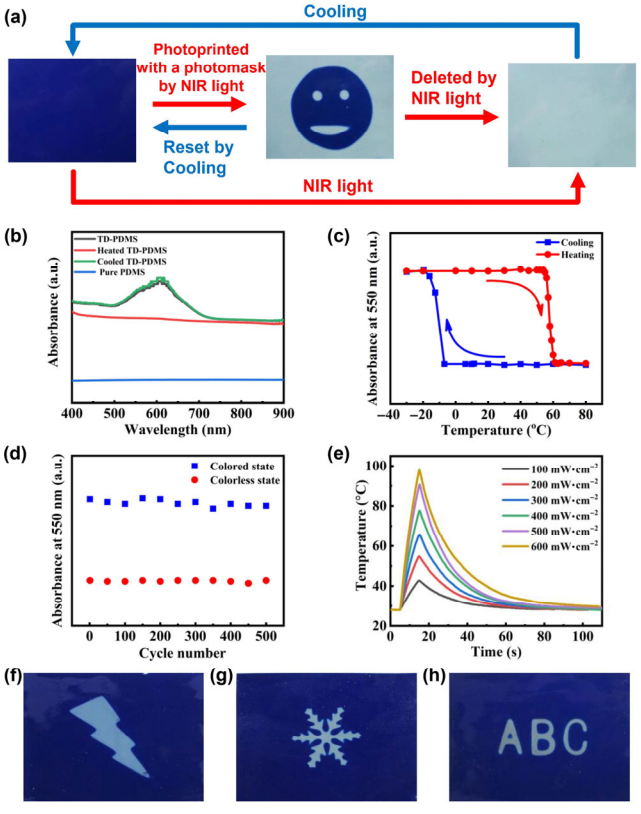


**Figure 3** (a) Schematic illustration of photoprinting or erasing patterns on the SACNT/TD-PDMS film. (b) Absorption spectra of the TD-PDMS composite (grey line), heated TD-PDMS composite (60 °C, red line), cooled TD-PDMS composite (−20 °C, green line), and pure PDMS (blue line). (c) Absorption spectrum showing the hysteresis characteristic of TD-PDMS composite. (d) Absorption spectrum of the TD-PDMS composite for 500 heating/cooling cycles. (e) Temperature of the SACNT/TD-PDMS film as a function of time under different light powers. (f)–(h) Optical photographs of patterns or English letters photoprinted on the SACNT/TD-PDMS film by using NIR light.

To further investigate the color-switching characteristics, the above TD-PDMS film was placed in different temperature environments (−30 to 80 °C, and 80 to −30 °C). The arrows in Fig. 3(c) indicate the temperature variation process. Figure 3(c) exhibits the trend of absorption intensity (wavelength at 550 nm) with different temperature. When the ambient temperature was below 60 °C, the TD-PDMS film maintained a blue color. It became colorless and such state could be maintained, when the temperature exceeded 60 °C. The TD-PDMS film remained colorless during the cooling process. It returned to the colored state (blue color) only in low temperature environment (< −20 °C). The above results show that the TD-PDMS film can keep the colored or colorless state in the normal temperature range (0 to 40 °C). Such bistable states are the working principle of the SACNT/TD-PDMS rewritable medium. Afterwards, the repeatability of the TD-PDMS film was studied. The film was placed under 65 and −25 °C repeatedly. As displayed in Fig. 3(d), the absorption intensity (550 nm) did not show significant degeneration during 500 cycles test. Therefore, the TD-PDMS film exhibits good repeatability for color-switching.

Using SACNT as the photothermal layer will greatly facilitate the usage of rewritable medium. The temperature of SACNT/TD-PDMS film increased rapidly, when the SACNT layer was illuminated by NIR light. When the temperature reached 60 °C, the color of TD-PDMS layer changed accordingly.

As shown in Fig. 3(e), the temperature of SACNT/TD-PDMS film changed with time under different light powers. Higher temperature of the composite film is caused by higher light power. If the patterns need to be photoprinted within 10 s, the required light power density should be higher than 300 mW·cm$^{-2}$. In other words, higher light power would lead to shorter photoprinting time.

Diversiform patterns can be photoprinted on the SACNT/TD-PDMS film by NIR light irradiation through the photomask. As shown in Figs. 3(f) and 3(g), the patterns of lightning or snowflake were photoprinted on the SACNT/TD-PDMS film. Not only clear patterns can be photoprinted, but also English letters can be clearly displayed on the SACNT/TD-PDMS film, as shown in Fig. 3(h). The SACNT/TD-PDMS film has good stretchability and flexibility. Its mechanical properties are shown in Fig. S2(a) in the ESM. Along the direction perpendicular to the SACNT alignment ($\alpha$ = 90°), the SACNT/TD-PDMS film can be easily stretched (maximum strain > 60%). The Young's modulus and tensile strength were 0.47 and 0.27 MPa respectively (Fig. S2(b) in the ESM). Along the direction parallel to the SACNT alignment ($\alpha$ = 0°), the composite film can hardly be stretched (maximum strain < 3%). The Young's modulus and tensile strength were 92.4 and 1.6 MPa respectively (Fig. S2(b) in the ESM). Meanwhile, when the SACNT/TD-PDMS film was stretched, the photoprinted pattern could still be clearly displayed (Fig. S3(a) in ESM). As shown in Fig. S3(b) in the ESM, the pattern also did not change after the folding of the composite film. Therefore, the SACNT/TD-PDMS composite film is able to be fixed at irregular parts without affecting the information displaying.

It should be noted that the patterns can be kept legible for at least 6 months (Fig. S4 in the ESM), demonstrating long legible time compared with other rewritable media. To demonstrate that the SACNT/TD-PDMS composite provides a long-term usage, it was exposed to NIR light for a long time. After 24 and 72 h of NIR light irradiation (200 mW·cm$^{-2}$) respectively, the mechanical properties of the SACNT/TD-PDMS composite were studied. The tensile stress-strain curves are shown in Fig. S5(a) in the ESM. Compared to the initial state (Fig. S2(b) in the ESM), the Young's modulus and the tensile strength showed no significant decrease (Fig. S5(b) in the ESM). Hence, after 72 h of continuous exposure to NIR light, the mechanical properties of the SACNT/TD-PDMS composite did not change obviously, and it was still stretchable in the direction perpendicular to SACNT alignment. It shows that the composite film can meet the practical application.

In a word, these results fully reveal the potential of SACNT/TD-PDMS film using as the flexible rewritable medium for information storage and display.

### 3.3 Actuation performance of the SACNT/TD-PDMS composite

Actuating materials have great potentials applications in artificial muscles, bionic devices, switches, robots, etc. As mentioned previously, the SACNT/TD-PDMS composite can be used as an actuator through tailoring. The length direction of the actuator should be along the SACNT alignment direction ($\alpha$ = 0°). Figure 4(a) schematically illustrates the morphing mechanism of SACNT/TD-PDMS actuator. After the preparation process, the embedded SACNT is still well-aligned in the polymer matrix (Fig. S1 in the ESM). Because the coefficient of thermal expansion (CTE) of the SACNT layer along the SACNT alignment is much smaller than that of the TD-PDMS layer, the actuator will bend toward the SACNT side when heated by NIR light. Owing to the introducing of TD, the CTE of TD-PDMS composite is smaller than that of pure PDMS. However, the SACNT/TD-PDMS actuator still showed visible morphing under NIR light irradiation. If the temperature of actuator is higher than 60 °C, the color of TD-PDMS layer changes. By turning off the NIR light, the actuator will return to its initial shape and its color remains the colorless state. Therefore, the color-switching phenomenon can serve to indicate the use trace of the actuator.

Figure 4(b) shows the bending-morphing of the actuator in different states, corresponding to Fig. 4(a). Note S2 and Fig. S6 in the ESM explain the calculation of bending curvature. The bending curvature is defined as a positive value, when the actuator bends to the SACNT side. In contrast, the curvature is defined as a negative value, when it bends to the TD-PDMS side. The actuator was initially in a relatively straight state (curvature of −0.19 cm$^{-1}$). When illuminated by NIR light (600 mW·cm$^{-2}$), the actuator showed bending morphing to the SACNT side in 10 s. The bending curvature was 0.43 cm$^{-1}$. When the NIR light source was taken away, the actuator shape would be recovered. Simultaneous measurements of bending curvature and temperature in the morphing course were carried out (Fig. 4(c)). When illuminated by NIR light (600 mW·cm$^{-2}$), the temperature of actuator rapidly increased from 28 to 98 °C in 10 s. The bending curvature and temperature gradually returned to the initial states after the NIR light was turned off.

The relationship between the maximum bending curvature and the light power is shown in Fig. 4(d). It can be seen that as the light power increased, the actuator would have higher temperature and larger bending-morphing. The relationship between the bending curvature and the temperature is also shown in Fig. S7 in the ESM. Furthermore, the morphing process was tested for 200 cycles repeatedly. As shown in Fig. 4(e), the

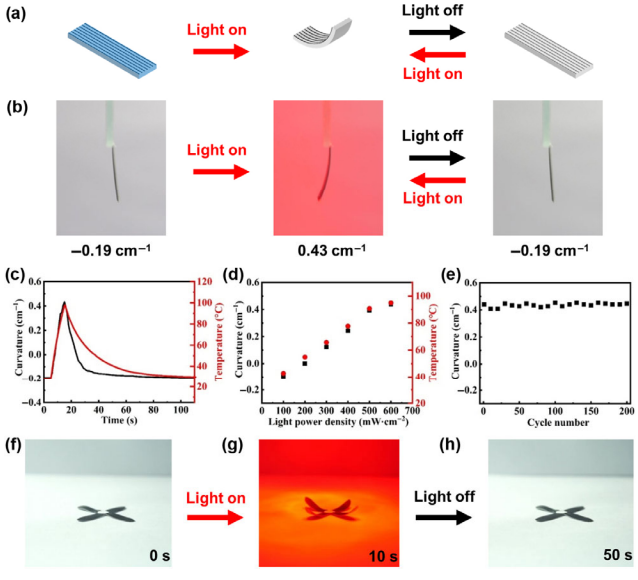


**Figure 4** (a) Schematic illustration of the light-driven actuation of SACNT/TD-PDMS actuator. (b) Optical photographs of the SACNT/TD-PDMS actuator before NIR light irradiation (left panel), under NIR light irradiation (600 mW·cm$^{-2}$) for 10 s (middle panel) and after NIR light irradiation (right panel). (c) Bending curvature (black curve) and temperature (red curve) of the SACNT/TD-PDMS actuator as a function of time. (d) Maximum bending curvature (black curve) and maximum temperature (red curve) of the SACNT/TD-PDMS actuator as a function of light power density. (e) Repeatability test of the SACNT/TD-PDMS actuator under repeated NIR light irradiation (600 mW·cm$^{-2}$). (f) Initial state of the bionic flower fabricated by SACNT/TD-PDMS actuators. (g) Bending-morphing process of the bionic flower under NIR light irradiation (600 mW·cm$^{-2}$). (h) Bionic flower returns back to the initial state.

maximum bending curvature almost maintained at 0.43 $cm^{-1}$, indicating good repeatability and durability of the SACNT/TD-PDMS actuator. Based on the characteristics of the SACNT/TD-PDMS actuator, a bionic flower was fabricated. The bionic flower was composed of four petals. The size of every petal was about 0.5 cm × 2 cm. When the bionic flower was placed on a table, the petals were flat initially (Fig. 4(f)). When illuminated by NIR light, the petals bent upwards (Fig. 4(g)). After turning off the NIR light, the bionic flower returned to the flat state (Fig. 4(h)).

In addition, the SACNT/TD-PDMS composites are prepared without using toxic or environmentally harmful materials and the preparation process is environmentally friendly. Meanwhile, the SACNT and TD are almost encapsulated by PDMS, which allows the composite to remain stable during utilization. When the SACNT/TD-PDMS composite is used, only the PDMS contacts the human body. As the PDMS has good biocompatibility, the SACNT/TD-PDMS composite is expected to be used in wearable devices, especially in smart clothing. We also notice that there were several reports about the use of actuating materials in smart clothing [19, 31]. For example, Mu et al. proposed an ambient-driven actuator and obtained a smart fabric with self-adaptive function [19]. When the temperature and humidity of human body change, the channel on the fabric can be opened or closed automatically, which helps to control the body moisture and skin temperature. We expect that the SACNT/TD-PDMS actuators can be applied in smart clothing. An example is designed as follows. At first, the human body is in a comfortable state under cool conditions. At this time, the SACNT/TD-PDMS actuators integrated in the clothing are in the flat state (Fig. S8(a) in the ESM). However, when the body is irradiated by strong sunlight or the ambient temperature increases, the human body needs to dissipate heat to the environment. Under such conditions, the SACNT/TD-PDMS actuators bend outward, thereby providing opening air holes for heat dissipation (Fig. S8(b) in the ESM). According to the actual situation, we can control the shape-morphing of SACNT/TD-PDMS actuators, so as to adjust the body temperature and make the clothing smart.

### 3.4 Sensing performance of the SACNT/TD-PDMS composite

The SACNT/TD-PDMS composite film is capable of being utilized as a strain sensor as well. The stretching property of the composite is demonstrated in Fig. S2(a) in the ESM. We can see that the composite can be hardly stretched in the direction along the SACNT alignment, but can be easily stretched in the direction perpendicular to the SACNT alignment. The unique anisotropy of SACNT results in such phenomenon. Figure 5(a) shows the photographs of SACNT/TD-PDMS composite under different strains. The composite film can withstand at least 20% applied strain, when it is stretched along the direction perpendicular to the SACNT alignment.

We further characterized the electrical resistance changes of SACNT/TD-PDMS sensor under different applied strains (5%, 10%, 15% and 20%). As shown in Fig. 5(b), the relative resistance change ($\Delta R/R_0$) increased as the strain increased, but the increasing was non-linear ($\Delta R = R - R_0$, $R$ is the resistance under different strains, and $R_0$ is the initial resistance without strain). The figure of merit to illustrate the sensitivity of sensor is the gauge factor (GF). The definition is $GF = \Delta R/(R_0\ \varepsilon)$, in which $\varepsilon$ means the strain. As shown in Fig. 5(c), the strain sensing curve is divided into three regions. The relative resistance change increased in the strain range of 0–2.8% with a GF of 4.56. When the strain continued to increase, the relative resistance change increased rapidly and the GF was 13.5, which can be explained by breaking the microcrack connection of SACNT layer under tensile stress. When the strain further increased to be larger than 9.5%, the relative resistance change slowed down and the GF was 1.86.

To explore the mechanism of strain sensing, we used an optical microscope to observe the surface morphology of SACNT/TD-PDMS sensor under different strains, as shown in Fig. 5(d). When no strain was applied, the SACNTs in the composite were bonded together to form a good conductive network. When a small strain was applied (region I in Fig. 5(c)),

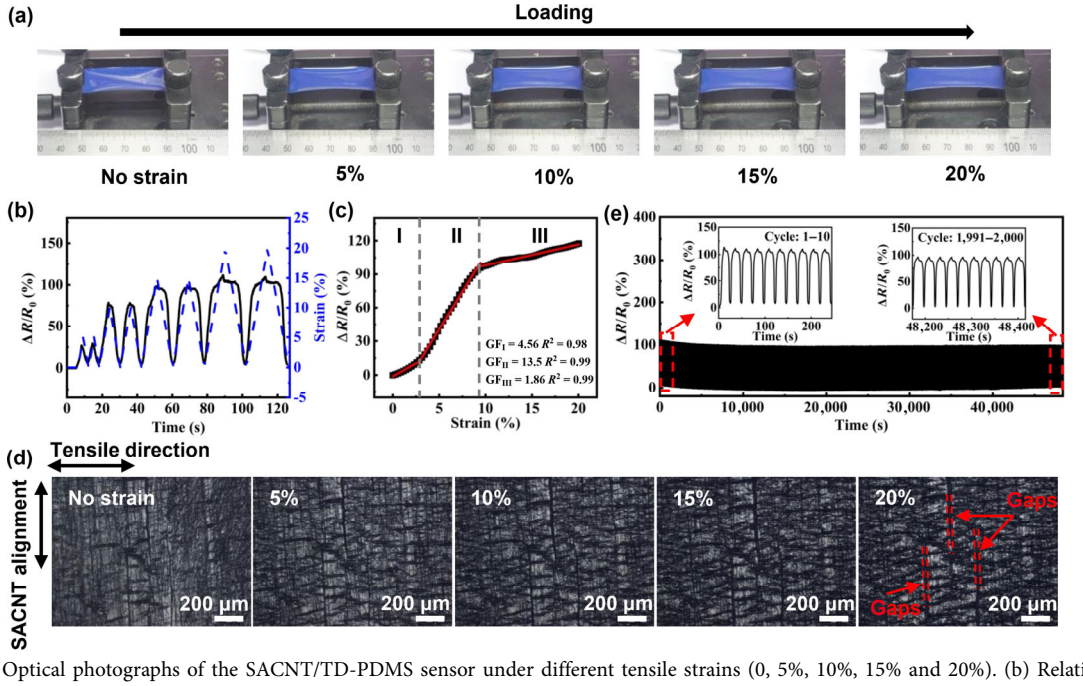


**Figure 5** (a) Optical photographs of the SACNT/TD-PDMS sensor under different tensile strains (0, 5%, 10%, 15% and 20%). (b) Relative resistance change under different tensile strains during the stretching-releasing process (tensile rate: 0.7 mm·$s^{-1}$). (c) Relative resistance change as a function of strain (tensile rate: 0.7 mm·$s^{-1}$). (d) Optical microscopic images of the SACNT surface under different tensile strains during stretching, corresponding to (a). (e) Repeatability test of the SACNT/TD-PDMS sensor under strain of 20% for 2,000 cycles (tensile rate: 0.7 mm·$s^{-1}$).

the SACNTs were still bonded together, allowing many possible electron paths. When a larger strain was applied (region II in Fig. 5(c)), the SACNTs started to separate from each other, resulting in fewer conduction paths in the stretching direction. As the strain continued to increase (region III in Fig. 5(c)), the resistance change became slower. Such phenomenon can be explained as follows. On one hand, the disconnection of the SACNT network is still the main factor according to the applied strain. On the other hand, the cross-sectional area reduces during stretching, which may raise the areal density of SACNTs. Therefore, the resistance would continue to increase during the stretching process, but the change rate would slow down. Similar resistance change phenomena were also reported in previous CNT-based sensors [9, 32, 33].

To compare with the SACNT/TD-PDMS composite, we also used disordered CNT (DCNT) to prepare the composite. The preparation method was similar to that of SACNT/TD-PDMS composite. More details of the experiment are in Note S1 in the ESM. The mechanical properties of the DCNT/TD-PDMS composite are shown in Fig. S9(a) in the ESM. Although the DCNT/TD-PDMS composite was also stretchable, the strain (< 25%) was much smaller than that of SACNT/TD-PDMS composite (> 60%) in the direction perpendicular to the SACNT alignment. As a large strain is required at some joints, relative small starin may affect the wearing comfort when the DCNT/TD-PDMS composite is used in wearable devices. As shown in Fig. S9(b) in the ESM, the sensing performance of the DCNT/TD-PDMS composite was also tested with a GF of 2.0, which was poorer than that of the SACNT/TD-PDMS composite (maximal GF of 13.5). Therefore, although the sensing function could also be achieved by using the DCNT, its strain and sensing performance were not as good as those by using the SACNT.

To test the sensing repeatability, the SACNT/TD-PDMS sensor was subjected to 2,000 cycles of tensile testing ($\varepsilon$ = 20%). As shown in Fig. 5(e), the sensor output stable sensing signals during the test. The interface between SACNT layer and TD-PDMS layer after the cycle test is shown in Fig. S10 in the ESM. There was no delamination at the interface after the cycling test. The above results demonstrate excellent stability of SACNT/TD-PDMS composites for practical sensing applications.

### 3.5 Applications of the SACNT/TD-PDMS composite

As mentioned in the previous sections, the SACNT/TD-PDMS composite is able to deliver the functions of rewriting, actuating and sensing respectively. We hope that these functions can be applied synergistically. As a proof of concept, we present two smart wearable devices fabricated by the SACNT/TD-PDMS composite, which demonstrate rewritable information display together with sensing function. As shown in Fig. 6(a), a customized pattern was photoprinted on the SACNT/TD-PDMS film and electrodes were embedded in the film in advance. Then, the composite film was attached onto a glove to fabricate a smart glove. When wearing the smart glove, the movement of hand could be detected by testing the electrical signals, as shown in Fig. 6(b). Initially, when the hand was in a relaxed state, the resistance of the smart glove did not change. When the hand turned to a fisted state, the smart glove was stretched and the resistance changed significantly. The pattern on the smart glove remained intact, although it was stretched during this process. Furthermore, the pattern on the smart glove could be replaced many times according to actual needs.

As another application example, a smart armband composed of two parts was prepared (Fig. 6(c)). The main part was the

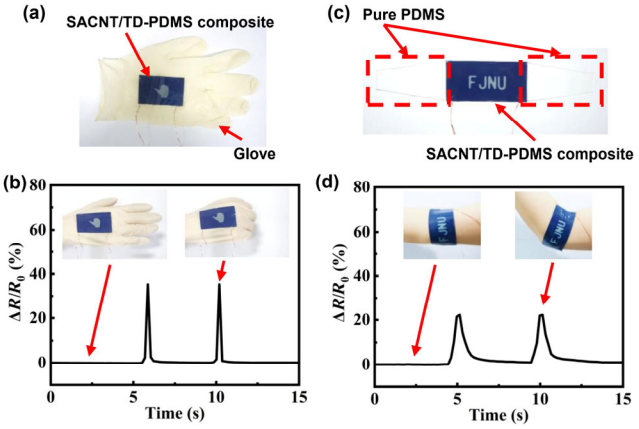


**Figure 6** (a) Optical photograph of the smart glove. (b) Using the smart glove to monitor hand movements. (c) Optical photograph of the smart armband. (d) Using the smart armband to monitor elbow movements.

SACNT/TD-PDMS composite for sensing and rewritable information display. The rest of pure PDMS part acted like a watch band. After wrapping the smart armband around the elbow, two ends of the pure PDMS part were overlapped. By placing two magnet stones on the overlapping part of pure PDMS, the smart armband with a customized photoprinted pattern was fixed firmly on the elbow (inset figure of Fig. 6(d)). Figure 6(d) shows the relative resistance change of the smart armband, which demonstrated the movement of elbow in real-time. Regular and periodic signals were observed obviously. Meanwhile, the English letters of "FJNU" could be clearly seen on the smart armband. This strategy can extend to fabricate other multifunctional wearable devices, which display the specified information while implementing the sensing function. The rewritable feature will enrich the life and usage scenarios of such multifunctional devices.

## 4 Conclusions

In summary, a facile method is proposed to prepare multifunctional wearable devices based on SACNT/TD-PDMS composite. By fully utilizing the characteristics of each component material, the composite film realizes three different functions. First, it can be used as a rewritable medium. Patterns can be repeatedly photoprinted on and erased from the flexible composite film. Second, the SACNT/TD-PDMS composite can be used as an actuating material, showing bending-morphing under NIR light illumination. We also put forward the concept of combining actuating materials with clothing to prepare a smart clothing. Third, the SACNT/TD-PDMS composite is able to be utilized as a strain sensor. Based on the above characteristics, we propose a strategy that both sensing and rewriting functions are realized in one monolithic SACNT/TD-PDMS composite film. Two wearable sensing devices capable of displaying information at the same time are demonstrated as application examples. With further development, this versatile SACNT/TD-PDMS composite is expected to have promising potentials in smart clothing, multifunctional appliances and next-generation wearable devices.

## Acknowledgements

This work was supported by the National Natural Science Foundation of China (Nos. 51773039 and 11974076), Natural Science Foundation of Fujian Province (Nos.2020J02036 and 2018J06001), Program for New Century Excellent Talents in University of Fujian Province (No. J1-1318), and Open Research

Fund Program of the State Key Laboratory of Low-Dimensional Quantum Physics (No. KF201810).

**Electronic Supplementary Material**: Supplementary material (SEM image of the SACNT surface of SACNT/TD-PDMS composite, mechanical properties of the SACNT/TD-PDMS composite, optical photographs of the SACNT/TD-PDMS composite before and after stretching/folding, optical photographs of the SACNT/TD-PDMS composite after different days, mechanical properties of the SACNT/TD-PDMS composite after long-time light irradiation, SACNT/TD-PDMS actuator with correlative parameters for calculating the bending curvature, bending curvature of SACNT/TD-PDMS actuator as a function of temperature, schematic diagram of smart clothing combined with SACNT/TD-PDMS actuators, mechanical properties of the DCNT/TD-PDMS composite, SEM image of the interface between SACNT layer and TD-PDMS layer after applying strain of 20% for 2,000 cycles, experimental details, bending curvature calculation principle of the SACNT/TD-PDMS actuator) is available in the online version of this article at https://doi.org/10.1007/s12274-020-3285-3.

## References


[1] Ma, Y. J.; Zhang, Y. C.; Cai, S. S.; Han, Z. Y.; Liu, X.; Wang, F. L.; Cao, Y.; Wang, Z. H.; Li, H. F.; Chen, Y. H. et al. Flexible hybrid electronics for digital healthcare. *Adv. Mater.* **2020**, *32*, 1902062.

[2] Trung, T. Q.; Lee, N. E. Flexible and stretchable physical sensor integrated platforms for wearable human-activity monitoring and personal healthcare. *Adv. Mater.* **2016**, *28*, 4338–4372.

[3] Wang, C. Y.; Xia, K. L.; Wang, H. M.; Liang, X. P.; Yin, Z.; Zhang, Y. Y. Advanced carbon for flexible and wearable electronics. *Adv. Mater.* **2019**, *31*, 1801072.

[4] Nozariasbmarz, A.; Suarez, F.; Dycus, J. H.; Cabral, M. J.; LeBeau, J. M.; Öztürk, M. C.; Vashaee, D. Thermoelectric generators for wearable body heat harvesting: Material and device concurrent optimization. *Nano Energy* **2020**, *67*, 104265.

[5] Ning, W.; Wang, Z. H.; Liu, P.; Zhou, D. L.; Yang, S. Y.; Wang, J. P.; Li, Q. Q.; Fan, S. S.; Jiang, K. L. Multifunctional super-aligned carbon nanotube/polyimide composite film heaters and actuators. *Carbon* **2018**, *139*, 1136–1143.

[6] Zhou, Z. W.; Yan, Q. H.; Liu, C. H.; Fan, S. S. An arm-like electrothermal actuator based on superaligned carbon nanotube/polymer composites. *New Carbon Mater.* **2017**, *32*, 411–418.

[7] Wang, W.; Xiang, C. X.; Zhu, Q.; Zhong, W. B.; Li, M. F.; Yan, K. L.; Wang, D. Multistimulus responsive actuator with go and carbon nanotube/PDMS bilayer structure for flexible and smart devices. *ACS Appl. Mater. Interfaces* **2018**, *10*, 27215–27223.

[8] Wang, L.; Chen, Y.; Lin, L. W.; Wang, H.; Huang, X. W.; Xue, H. G.; Gao, J. F. Highly stretchable, anti-corrosive and wearable strain sensors based on the PDMS/CNTs decorated elastomer nanofiber composite. *Chem. Eng. J.* **2019**, *362*, 89–98.

[9] Tas, M. O.; Baker, M. A.; Masteghin, M. G.; Bentz, J.; Boxshall, K.; Stolojan, V. Highly stretchable, directionally oriented carbon nanotube/PDMS conductive films with enhanced sensitivity as wearable strain sensors. *ACS Appl. Mater. Interfaces* **2019**, *11*, 39560–39573.

[10] Otley, M. T.; Zhu, Y. M.; Zhang, X. Z.; Li, M. F.; Sotzing, G. A. Color-tuning neutrality for flexible electrochromics via a single-layer dual conjugated polymer approach. *Adv. Mater.* **2014**, *26*, 8004–8009.

[11] Wang, W. S.; Liu, L. T.; Feng, J.; Yin, Y. D. Photocatalytic reversible color switching based on titania nanoparticles. *Small Methods* **2018**, *2*, 1700273.

[12] Zhu, P. C.; Wang, Y. L.; Wang, Y.; Mao, H. Y.; Zhang, Q.; Deng, Y. Flexible 3D architectured piezo/thermoelectric bimodal tactile sensor array for E-skin application. *Adv. Energy Mater.* **2020**, *10*, 2001945.

[13] Amjadi, M.; Sitti, M. Self-sensing paper actuators based on graphite-carbon nanotube hybrid films. *Adv. Sci.* **2018**, *5*, 1800239.

[14] Zhong, J. W.; Ma, Y.; Song, Y.; Zhong, Q. Z.; Chu, Y.; Karakurt, I.; Bogy, D. B.; Lin, L. W. A flexible piezoelectret actuator/sensor patch for mechanical human-machine interfaces. *ACS Nano* **2019**, *13*, 7107–7116.

[15] Xiao, P.; Liang, Y.; He, J.; Zhang, L.; Wang, S.; Gu, J. C.; Zhang, J. W.; Huang, Y. J.; Kuo, S.; Chen, T. Hydrophilic/hydrophobic interphase-mediated bubble-like stretchable Janus ultrathin films toward self-adaptive and pneumatic multifunctional electronics. *ACS Nano* **2019**, *13*, 4368–4378.

[16] Wang, X. Q.; Chan, K. H.; Cheng, Y.; Ding, T. P.; Li, T. T.; Achavananthadith, S.; Ahmet, S.; Ho, J. S.; Ho, G. W. Somatosensory, light-driven, thin-film robots capable of integrated perception and motility. *Adv. Mater.* **2020**, *32*, 2000351.

[17] Ma, C. X.; Lu, W.; Yang, X. X.; He, J.; Le, X. X.; Wang, L.; Zhang, J. W.; Serpe, M. J.; Huang, Y. J.; Chen, T. Bioinspired anisotropic hydrogel actuators with on-off switchable and color-tunable fluorescence behaviors. *Adv. Funct. Mater.* **2018**, *28*, 1704568.

[18] Wang, Y. L.; Cui, H. Q.; Zhao, Q. L.; Du, X. M. Chameleon-inspired structural-color actuators. *Matter* **2019**, *1*, 626–638.

[19] Mu, J. K.; Wang, G.; Yan, H. P.; Li, H. Y.; Wang, X. M.; Gao, E. L.; Hou, C. Y.; Pham, A. T. C.; Wu, L. J.; Zhang, Q. H. et al. Molecular-channel driven actuator with considerations for multiple configurations and color switching. *Nat. Commun.* **2018**, *9*, 590.

[20] Cai, G. F.; Wang, X.; Cui, M. Q.; Darmawan, P.; Wang, J. X.; Eh, A. L. S.; Lee, P. S. Electrochromo-supercapacitor based on direct growth of NiO nanoparticles. *Nano Energy* **2015**, *12*, 258–267.

[21] Yun, T. Y.; Li, X. L.; Kim, S. H.; Moon, H. C. Dual-function electrochromic supercapacitors displaying real-time capacity in color. *ACS Appl. Mater. Interfaces* **2018**, *10*, 43993–43999.

[22] Wu, X. M.; Wang, Q. G.; Zhang, W. Z.; Wang, Y.; Chen, W. X. Enhanced electrochemical performance of hydrogen-bonded graphene/polyaniline for electrochromo-supercapacitor. *J. Mater. Sci.* **2016**, *51*, 7731–7741.

[23] Jiang, K. L.; Li, Q. Q.; Fan, S. S. Spinning continuous carbon nanotube yarns. *Nature* **2002**, *419*, 801.

[24] Zhang, X.; Jiang, K.; Feng, C.; Liu, P.; Zhang, L.; Kong, J.; Zhang, T.; Li, Q.; Fan, S. Spinning and processing continuous yarns from 4-inch wafer scale super-aligned carbon nanotube arrays. *Adv. Mater.* **2006**, *18*, 1505–1510.

[25] Feng, C.; Liu, K.; Wu, J. S.; Liu, L.; Cheng, J. S.; Zhang, Y. Y.; Sun, Y. H.; Li, Q. Q.; Fan, S. S.; Jiang, K. L. Flexible, stretchable, transparent conducting films made from superaligned carbon nanotubes. *Adv. Funct. Mater.* **2010**, *20*, 885–891.

[26] Jiang, K. L.; Wang, J. P.; Li, Q. Q.; Liu, L.; Liu, C. H.; Fan, S. S. Superaligned carbon nanotube arrays, films, and yarns: A road to applications. *Adv. Mater.* **2011**, *23*, 1154–1161.

[27] Yu, Y.; Luo, S.; Sun, L.; Wu, Y.; Jiang, K. L.; Li, Q. Q.; Wang, J. P.; Fan, S. S. Ultra-stretchable conductors based on buckled super-aligned carbon nanotube films. *Nanoscale* **2015**, *7*, 10178–10185.

[28] Chen, L. Z.; Weng, M. C.; Zhou, Z. W.; Zhou, Y.; Zhang, L. L.; Li, J. X.; Huang, Z. G.; Zhang, W.; Liu, C. H.; Fan, S. S. Large-deformation curling actuators based on carbon nanotube composite: Advanced-structure design and biomimetic application. *ACS Nano* **2015**, *9*, 12189–12196.

[29] Chen, L. Z.; Weng, M. C.; Zhang, W.; Zhou, Z. W.; Zhou, Y.; Xia, D.; Li, J. X.; Huang, Z. G.; Liu, C. H.; Fan, S. S. Transparent actuators and robots based on single-layer superaligned carbon nanotube sheet and polymer composites. *Nanoscale* **2016**, *8*, 6877–6883.

[30] Chen, L. Z.; Weng, M. C.; Huang, F.; Zhang, W. Long-lasting and easy-to-use rewritable paper fabricated by printing technology. *ACS Appl. Mater. Interfaces* **2018**, *10*, 40149–40155.

[31] Shi, Q. W.; Li, J. H.; Hou, C. Y.; Shao, Y. L.; Zhang, Q. H.; Li, Y. G.; Wang, H. Z. A remote controllable fiber-type near-infrared light-responsive actuator. *Chem. Commun.* **2017**, *53*, 11118–11121.

[32] Zhou, J.; Yu, H.; Xu, X. Z.; Han, F.; Lubineau, G. Ultrasensitive, stretchable strain sensors based on fragmented carbon nanotube papers. *ACS Appl. Mater. Interfaces* **2017**, *9*, 4835–4842.

[33] Chen, S. J.; Wu, R. Y.; Li, P.; Li, Q.; Gao, Y.; Qian, B.; Xuan, F. Z. Acid-interface engineering of carbon nanotube/elastomers with enhanced sensitivity for stretchable strain sensors. *ACS Appl. Mater. Interfaces* **2018**, *10*, 37760–37766.